

Control of Ion Energy in a Capacitively Coupled Reactive Ion Etcher

H. M. Park*, C. Garvin, D. S. Grimard and J. W. Grizzle

Electronics Manufacturing and Control Systems Laboratory,
Dept. of Electrical Engineering and Computer Science, University of Michigan,
Ann Arbor, MI 48109-2122, USA

ABSTRACT

The energy of ions bombarding the wafer is proportional to the potential difference between the plasma and the powered electrode in Reactive Ion Etching (RIE) systems. This work seeks to control the ion energy without altering the applied RF power or the chamber pressure since these variables are closely tied to other important quantities, such as reactive chemical species concentrations in the plasma and wafer etch uniformity. A variable resistor placed in parallel with the blocking capacitor allows the plasma self bias voltage (V_{bias}) to be arbitrarily varied between its nominal value and zero. Optical emission spectroscopy for a CF_4 plasma reveals that the nominal plasma chemical concentrations do not change under this control method. The use of a Langmuir probe to measure the plasma potential shows that the ion energy changes by approximately one half of the change in V_{bias} . The potential uses of this ion energy control technique to plasma self bias voltage regulation, etch selectivity and plasma cleaning of chamber walls are demonstrated. A potential drawback, namely decreased plasma stability, is also indicated.

*Author to whom correspondence should be addressed. email: parkhm@engin.umich.edu

1 Introduction and Background

Reactive Ion Etching (RIE) is the dominant etching process for the transfer of fine features from masks to wafers. It is well known that ion bombardment plays an important role in the creation of anisotropic profiles, etch rate enhancement and surface damage [1–3] and hence significant research has been dedicated to the control of the ion bombardment energy in RIE systems [4–8]. In standard capacitively coupled RIE systems, the conventional approach to ion energy control has been through chamber pressure or applied RF power. The drawbacks are that changing power also alters the chemical concentrations in the plasma and changing pressure will affect the uniformity of the etching process across the wafer [9, 10]. In part, to overcome these drawbacks, new types of plasma sources have been developed so that ion energy can be controlled independently of the chemical concentration and chamber pressure. These include Electron Cyclotron Resonance (ECR), helicon, helical resonator, Transformer Coupled Plasma (TCP), and Inductive Plasma Source (IPS), which operate in low pressure and high plasma density range [11–14].

This paper is exclusively concerned with ion energy control in classical capacitively coupled RIE systems. Figure 1 is a schematic of a typical parallel plate RIE system along with a corresponding electrical potential from anode to cathode. In an asymmetric RIE system (smaller powered electrode area than grounded electrode area), the presence of a blocking capacitor leads to a large negative plasma self bias voltage (V_{bias}) being induced on the powered electrode. The time-averaged plasma potential (V_p) can be estimated as [15]

$$V_p = \frac{V_{rf} + V_{bias}}{2}, \quad (1)$$

where V_{rf} is the peak amplitude of the applied voltage of the RF generator power. Ions bombard the wafer surface due to the potential difference between the plasma and the powered electrode, and this potential difference defines the average ion energy (\mathcal{E}_{ion}) in a collisionless sheath via

$$\mathcal{E}_{ion} = q \cdot (V_p - V_{bias}), \quad (2)$$

where q is the charge of an ion [16]. The plasma potential (V_p) is an equipotential across the bulk plasma. In comparison to V_{bias} , V_p is rather small in magnitude, and therefore, V_{bias} is traditionally used to represent ion energy.

Several different techniques can be found in the literature for the control of ion energy to increase etch rate [4, 5], or selectivity [6, 7], to produce a positively tapered etch profile [8] or to minimize radiation damage [17]. The most common approach for the control of ion energy has been DC-biasing of the powered electrode. Nagy [4] increased the ion energy by adding a negative DC bias to the powered electrode, resulting in increased etch rate of polysilicon and SiO_2 . In his experiment, the plasma potential was slightly decreased with the addition of the negative DC bias; however, the ion energy, $V_p - V_{bias}$, increased proportionally to the applied DC bias voltage after the applied DC voltage exceeds a few tens of volts. Tai *et al.* used a zener diode tied to the blocking capacitor to control the ion energy [6]. Tai achieved a 50% selectivity improvement of SiO_2 to HPR-206 photoresist by increasing (i.e. decreasing its magnitude) of the V_{bias} from -470 V to -250 V in CHF_3 plasma.

The method used in this paper to control ion bombardment energy is related to [6]. As shown in Fig. 1, in a conventional RIE system, the net Direct Current (DC) through the powered electrode must be zero due to the DC blocking capacitor.

However, if a variable resistor is connected to the powered electrode as shown in Fig. 2, then the net DC is no longer forced to be zero. We observed that the V_{bias} developed at the powered electrode increases (i.e. decreases in magnitude) as the DC settles to a nonzero value. The result is that the V_{bias} can be controlled by regulating the amount of DC and thus can be manipulated by a variable resistor. From the definition of ion energy (2), an increase of V_{bias} by the use of a variable resistor will decrease the ion energy if the V_p is not varied during the control of the variable resistor.

To better understand the effects of this variable resistor on ion energy, it is helpful to analyze two extreme cases illustrated in Fig. 3: a) If the variable DC resistance is set to ∞ , then the system reduces to a conventional RIE system with $V_{bias} = V_{bias}^{nom}$ and $\mathcal{E}_{ion} = q \cdot (V_p^{nom} - V_{bias}^{nom})$; b) If the DC resistance is zero, then the system turns into a DC coupled RIE system with $V_{bias} = 0$ and $\mathcal{E}_{ion} = q \cdot V_p$. In the latter case, the higher mobility of the electrons leads to electron current dominating the DC through the electrodes. The higher efflux of electrons than ions from the plasma will lead to an increase in the plasma potential. This is illustrated in Fig. 3, where the plasma potential in a DC coupled RIE system is much higher than in a capacitively coupled system, and its lowest value does not approach zero [15, 18]. Therefore, the increase in the plasma potential acts as a limiting factor in ion energy control by this method. The amount of change in ion energy that can be obtained by this method is investigated in Section 4.1.

Two applications of ion energy control by the use of a variable resistor are explored in this paper. In the first one, the selectivity of polysilicon with respect to SiO_2 is investigated. It is known that the etch rate of polysilicon depends more on the concentration of the reactive chemical species (chemical etching) than the ion

energy (physical etching); in contrast to this, the etch rate of SiO_2 depends more strongly on the ion energy than the chemical reaction [16, 19, 20]. Therefore, in order to increase the selectivity of polysilicon to SiO_2 , the ion energy should be decreased while the reacting chemical concentration is either increased or kept constant. This work is presented in Section 4.2. Section 4.3 investigates an application of the ion energy control technique to an ion enhanced cleaning process. Polymer buildup on the etching chamber wall is regarded as a significant disturbance to the etching process and has been correlated to reduced device performance and yield [21–23]. By increasing the plasma potential, the ion bombardment energy toward the grounded wall will be increased, possibly enhancing a plasma cleaning process.

2 Experimental Setup

The experiment to measure the plasma potential with a Langmuir probe and the selectivity enhancement experiment were performed on a Gaseous Electronics Conference (GEC) reference cell that is described in detail in [24, 25]. The schematic of the experimental apparatus is shown in Fig. 4. The GEC is an RIE system having parallel, four-inch diameter, one-inch spaced, water-cooled stainless steel electrodes, housed in a stainless steel chamber. Vacuum is established by a mechanical pump and a turbo pump connected to the bottom of the chamber and pressure is controlled through a butterfly throttle valve.

Pressure is measured by an MKS type 127A baratron capacitive manometer. RF power at 13.56 MHz is supplied by an ENI ACG-5 power supply to the bottom electrode through an ENI MW-5 matching network. A Werlatone C1373 directional

coupler placed between the matching network and the powered electrode is used to measure forward (V^+) and reverse voltage (V^-) from which the power deposited into the plasma can be determined as

$$P_{deposited} = P_{forward} - P_{reverse} = \frac{|V^+|^2 - |V^-|^2}{Z_o} \quad (3)$$

where $P_{deposited}$ is the actual power deposited in the RIE system, $P_{forward}$ is the power supplied to the RIE system by the power supply, $P_{reverse}$ is the reflected power from the RIE system due to the impedance mismatch, and Z_o is a constant characteristic impedance, which is 50Ω in our experiment [26]. The upper electrode and chamber wall are grounded. The flow rate of plasma feed gas is controlled by an MKS mass flow controller and distributed through a showerhead arrangement in the upper electrode.

In order to mitigate any RF fluctuation when measuring the plasma potential relative to ground with a Langmuir probe, a tuned probe was constructed so that the impedance of the plasma to probe sheath is small in comparison to the probe to ground impedance at 13.56 MHz. The probe to ground impedance was increased by a pair of inductors which are self-resonant at 13.56 MHz along with the probe's parasitic capacitance. The cylindrical probe tip is made of tungsten and is placed at the midpoint between the two electrodes. The probe is controlled by an automated data acquisition system which is connected to a computer. A more detailed description can be found in [27–29]. The selectivity experiment was performed in a CF_4 plasma with 4% pre-mixed O_2 on unpatterned quarter slices of four-inch polysilicon and SiO_2 wafers. The wafers slices were placed on the powered electrode and etched at the same time. Film thicknesses before and after etching were determined by off-line ellipsometry measurements. The etch rate was calculated by dividing the thickness

of the film removed by the etch time. A National Instrument’s Data Acquisition (DAQ) card and LabVIEW software were used to acquire data and control the generator power, gas flow rate, pressure and the variable resistor at a 4 Hz sampling frequency.

The fluorine concentration measurement and ion enhanced cleaning experiments were performed on an Applied Materials 8300 (AME-8300) RIE system, described in detail in [30,31]. The AME-8300 is a hexode type RIE system, where wafers are placed vertically on a hexagonal powered electrode and an aluminum bell jar acts as the grounded electrode. The AME-8300 is equipped with an Optical Emission Spectroscopy (OES) system to monitor the intensity of the fluorine 703.7 nm emission line (I_F) and the intensity of the argon 750.4 nm emission line (I_{Ar}). These emissions are used to estimate fluorine concentration as $[F] = k \cdot (I_F/I_{Ar}) \cdot P$, where k is a proportionality constant and P is pressure. This RIE has also been equipped with a spectral reflectometry sensor system for determining a real-time film thickness and etch rate. Both of these systems are described in more detail in [32].

3 Variable Resistor Implementation and Control

The variable resistor illustrated in Fig. 5 was implemented by an enhancement mode p-MOSFET (breakdown voltage: 500 V). In order to minimize RF power dissipation through the variable resistor and to minimize RF “propagation noise,” an L-C filter was employed. The filter provides 30 dB attenuation at 13.56 MHz.

Typically, the magnitude of V_{bias} is larger than 100 V, and thus, the enhancement mode p-MOSFET is operating in its saturation region. Therefore, the drain-to-source resistance (R_{DS}) of the MOSFET is

$$R_{DS} = \frac{V_{DS}}{I_{DS}} = \frac{V_{DS}}{k \cdot (V_{GS} - V_T)^2}, \quad (4)$$

where V_{DS} is the drain to source voltage, I_{DS} is the drain to source current, k is a device dependent constant, V_{GS} is the gate bias voltage, and V_T is the threshold voltage. The total resistance of the variable resistor (R_{VAR}) is

$$R_{VAR} = \frac{(R_2 + R_3) \cdot [(R_1 + R_{DS})(R_2 + R_3) + R_1 \cdot R_{DS}]}{(R_2 + R_3)(R_1 + R_2 + R_3 + 2 \cdot R_{DS}) + R_1 \cdot R_{DS}}. \quad (5)$$

With the assumption of $R_{DS} \ll (R_2 + R_3)$ and $R_1 \ll (R_2 + R_3)$, (5) can be approximated as

$$R_{VAR} \simeq R_1 + R_{DS} \simeq \frac{V_{bias}}{k \cdot (V_{GS} - V_T)^2}. \quad (6)$$

Therefore, when V_{DS} is above the saturation voltage, the variable resistance can be controlled by the gate bias voltage (V_{GS}). In this study, $R_1=1 \text{ K}\Omega$, $R_2=40 \text{ M}\Omega$ and $R_3=1 \text{ M}\Omega$ were used, which yield a variable resistance range of 1 K – 20.5 M Ω for R_{VAR} . V_{bias} can be measured through the resistive voltage divider, R_2 and R_3 , which has a ratio 40:1.

A two-input two-output, decentralized controller was designed to regulate V_{bias} and the deposited power in the plasma to desired, constant setpoints with zero steady state error. As described in the experimental setup, the deposited power was

determined from a directional coupler placed near the powered electrode and V_{bias} was measured by the voltage divider of the variable resistor circuit described above. On the basis of these measurements, the controller adjusts the gate bias voltage of the p-MOSFET (i.e. regulating the variable resistor) and the RF generator power in order to control V_{bias} and deposited power to desired levels. Figure 6 shows an actual run of the controller on the GEC, where the desired setpoints for V_{bias} and deposited power were varied one at a time. The experiment was performed on the GEC at 30 sccm CF_4 with 4% pre-mixed O_2 and the pressure was held constant at 4.0 Pa with the standard MKS pressure controller. Due to the process interaction between deposited power and V_{bias} , it follows that an increase in deposited power causes V_{bias} to decrease (i.e. increase in the magnitude of V_{bias}). The gate bias voltage regulating V_{bias} reacts to compensate for the V_{bias} error by decreasing the resistance. The other interaction, an increase of V_{bias} changing the deposited power, is seen to be less significant. This controller was used in all of the experiments reported in the next section.

4 Experimental Results

4.1 V_{bias} and Ion Energy vs. Plasma Potential

In order to determine the relative value of the plasma potential as a function of the controlled V_{bias} , Langmuir probe measurements were performed on the GEC. Figure 7 is a plot of measured plasma potential as a function of V_{bias} under several operating conditions. As described in the published literature, the plasma potential increases slightly with increased deposited power under fixed pressure due to the

increased electron temperature [18] and as illustrated by Fig. 7 the plasma potential shows a relatively large dependence on the pressure under fixed deposited power. As previously discussed in Section 1, the plasma potential is increased with an increase of V_{bias} . The change in plasma potential from its nominal value (V_p^{nom}) under V_{bias} control is seen in Fig. 7 to be a nearly linear function of the variation in V_{bias} from its nominal value (V_{bias}^{nom}). From (1) and Fig. 7, the plasma potential under ion energy control is modified from (1) to

$$V_p \approx \frac{V_{bias}^{nom} + V_{rf}^{nom}}{2} + m(P) \cdot \Delta V_{bias}, \quad (7)$$

where,

V_p	plasma potential
V_{bias}^{nom}	nominal V_{bias} without ion energy control
V_{rf}^{nom}	nominal V_{rf} without ion energy control
ΔV_{bias}	$V_{bias} - V_{bias}^{nom}$
$m(P)$	pressure dependent slope

From the Fig. 7, the slope $m(P)$ is calculated as ≈ 0.5 for 33.3 Pa and ≈ 0.6 for 4.0 Pa. In this paper, we simply express the plasma potential under ion energy control as (8) for simplicity and ease of manipulation.

$$V_p \approx \frac{V_{bias}^{nom} + V_{rf}^{nom}}{2} + \frac{\Delta V_{bias}}{2}, \quad (8)$$

Figure 8 shows the comparison of two models of the plasma potential: model I based on (1); and model II based on (8). Since the plasma potential is increased by approximately one half of the V_{bias} change, it follows that the ion energy (\mathcal{E}_{ion}),

which is proportional to the potential difference between the plasma and the powered electrode, is changed by about one half of the V_{bias} change.

$$\Delta\mathcal{E}_{ion} = \Delta V_p - \Delta V_{bias} \approx \frac{-\Delta V_{bias}}{2}. \quad (9)$$

4.2 V_{bias} vs. Selectivity Enhancement

The goal for this part of the study was to investigate the selectivity enhancement by reducing the ion energy. First, it was necessary to demonstrate that the reactive radical species concentration in the plasma, and hence the chemical etching component of the RIE, was not affected by the ion energy controller. An actinometry sensor was used to record the fluorine concentration during V_{bias} control. Figure 9 shows that the fluorine concentration (arbitrary units) was unaffected by V_{bias} control, when the flow rate, deposited power and pressure were held constant. It follows that the chemical etching component should be essentially unchanged. The selectivity enhancement experiment was performed on the GEC cell at 30 sccm CF_4 with 4% pre-mixed O_2 and 33.3 Pa pressure. The deposited power of 16 W, which corresponds to a generator power of 50 W, was selected to provide -100 V plasma self bias voltage. At this operating point, the polysilicon etch rate was 5.2 (nm/min) whereas the etch rate of SiO_2 was 5.0 (nm/min), with a resulting selectivity of approximately 1.04. The V_{bias} was then controlled to -60 V. The polysilicon etch rate remained 5.2 (nm/min) while the SiO_2 etch rate decreased to 4.0 (nm/min). This yielded a selectivity of 1.30, and thus a 30% improvement in the selectivity of polysilicon to SiO_2 . By (9), the 40 V change in V_{bias} results in a net ion energy change of 20 eV. The decrease in SiO_2 etch rate can be explained from the change in ion energy: an approximately 20% drop in ion energy without changing chemical concentration

gives 20% decrease in SiO₂ etch rate. This is consistent with the results presented in [33] for dual source systems.

To achieve higher selectivity, it is necessary to further increase V_{bias} (i.e., decrease its magnitude). However, even if the V_{bias} is increased to zero, the ion energy will only be cut in half. In addition, the amount by which the V_{bias} voltage can be increased is limited by another factor. As the plasma potential is increased, arcing can occur between the plasma and the grounded surfaces (grounded electrode and wall). The point at which this occurs was observed to depend on the state (cleanliness) of the chamber wall. The typical controllable range of V_{bias} without any plasma instability was about 60 V in the GEC and 100 V in the AME-8300 from their nominal values. Finally, if the plasma potential becomes too high, the energetic ion bombardment on the grounded wall surfaces during an etch may result in contaminants being sputtered onto the wafer.

4.3 Ion Enhanced Cleaning Process

Recall that the Langmuir probe measurements revealed that increasing the V_{bias} to reduce ion bombardment energy at the wafer increases the plasma potential. This in turn increases the ion bombardment energy to the grounded surfaces, potentially creating a mechanism to enhance plasma cleaning efficiency. To test this hypothesis, a wafer holder was mounted on the chamber wall of the AME-8300 RIE system. A plasma with 30 sccm CHF₃, 2.7 Pa and 500 W deposited power was used to deposit polymer on a blanket silicon wafer inserted into the wall-mounted wafer holder. No bias control was used. After 30 minutes, the wafer was removed from the chamber and the polymer film thickness was measured on an ellipsometer. The wafer was then replaced on the chamber wall, and a plasma clean was run, with no bias control,

10 sccm O₂, 10 sccm Ar , 4.0 Pa and 250 W deposited power. The nominal V_{bias} was -187 V. The wafer was then removed again from the chamber and the cleaning rate was determined to be 65 Å/min. The same procedure was then followed, this time with various amounts of V_{bias} control applied. The results are summarized in Fig. 10. The cleaning rate as a function of V_{bias} shows a 25% improvement in cleaning rate with a 100 V increase in V_{bias} on the AME-8300 RIE system.

5 Conclusion

A novel ion energy control technique has been studied for capacitively coupled RIE systems. A variable resistor placed in parallel with the blocking capacitor allows the plasma self bias voltage, V_{bias} , to be varied from its nominal value to zero. The net change in ion energy that can be achieved with this method is approximately one half of the change in V_{bias} . This limitation is due to an increase in the plasma potential as the net DC flow around the blocking capacitor is varied. Two applications of controlling ion energy by this method were studied: polysilicon to SiO₂ selectivity enhancement and an ion enhanced plasma cleaning process. In the first case, a 30% improvement in selectivity was shown to be possible, and in the second, a 25% improvement in cleaning rate was demonstrated.

Acknowledgments

The authors sincerely thank S. Shannon (Univ. of Michigan) for help with the Langmuir probe measurements, Prof. M. Brake (Univ. of Michigan) for use of the GEC and Dr. H. Maynard (Lucent Technology) for useful discussions and suggestions. This work was supported in part by the Semiconductor Research Corporation under contract No. 96-FC-085, 97-FC-085 and by an AFOSR/DARPA MURI project under grant No. F49620-95-1-0524.

References

- [1] J. W. Coburn, *J. Vac. Sci. Technol. A* **12**, 1417 (1994).
- [2] K. P. Giapis, N. Sadeghi, J. Margot, R. A. Gottscho, and T. C. J. Lee, *J. Appl. Phys.* **73**, 7188 (1993).
- [3] R. H. Bruce, *Solid State Technol.* **24**, 64 (1981).
- [4] A. G. Nagy, *Solid State Technol.* **26**, 173 (1983).
- [5] H. Kawata, K. Murata, and K. Nagami, *J. Electrochem. Soc.* **132**, 206 (1985).
- [6] K. L. Tai and F. Vratny, Method for fabricating devices with dc bias-controlled reactive ion etching, US patent No. 4,496,448, 1985.
- [7] J. Brčka and R. Harman, *Vacuum* **36**, 531 (1986).
- [8] R. H. Bruce and A. R. Reinberg, *J. Electrochem. Soc.* **129**, 393 (1982).
- [9] J. L. Mauer and J. S. Logan, *J. Vac. Sci. Technol.* **16**, 404 (1979).
- [10] A. S. Kao and G. S. Stenger, Jr., *J. Electrochem. Soc.* **137**, 954 (1990).
- [11] M. A. Lieberman and A. J. Lichtenberg, *Principles of Plasma Discharges and Materials Processing*, p. 387, Wiley-Interscience, New York, 1994.
- [12] Y. Ra, S. G. Bradley, and C. H. Chen, *J. Vac. Sci. Technol. A* **12**, 1328 (1994).
- [13] H. H. sawin, *Microelectronic Engineering* **23**, 15 (1994).
- [14] J. H. Keller, *Plasma Sources Sci. Technol.* **5**, 166 (1996).
- [15] B. Chapman, *Glow Discharge Processes: Sputtering and Plasma Etching*, p. 145, Wiley-Interscience, New York, 1980.

- [16] J. Ding, J. S. Jenq, G. H. Kim, H. L. Maynard, J. S. Hamers, N. Hershkowitz, and J. W. Taylor, *J. Vac. Sci. Technol. A* **11**, 1283 (1993).
- [17] T. Arikado and Y. Horiike, *Jpn. J. Appl. Phys.* **22**, 799 (1983).
- [18] K. Köhler, J. W. Coburn, D. E. Horne, E. Kay, and J. H. Keller, *J. Appl. Phys.* **57**, 59 (1985).
- [19] G. Fortuño, *Plasma Chem. Plasma Process.* **8**, 19 (1988).
- [20] Y. H. Lee and M. Chen, *J. Appl. Phys.* **54**, 5966 (1983).
- [21] Y. H. Lee, G. S. Oehrlein, and C. Ransom, *Radiation Effects and Defects in Solids* **111-112**, 221 (1989).
- [22] S. Watanabe, *Jpn. J. Appl. Phys.* **31**, 1491 (1992).
- [23] K. Ino, I. Natori, A. Ichikawa, R. N. Vrtis, and T. Ohmi, *IEEE Trans. Semiconduct. Manufact.* **9**, 230 (1996).
- [24] J. K. Olthoff and K. E. Greenberg, *J. Res. Natl. Inst. Stand. Technol.* **100**, 327 (1995).
- [25] P. Hargis, Jr., K. E. Greenberg, P. A. Miller, J. B. Gerardo, J. R. Torczynski, M. E. Riley, G. A. Hebner, J. R. Roberts, J. K. Olthoff, J. R. Whetstone, R. J. V. Brunt, M. A. Sobolewski, H. M. Anderson, M. P. Splichal, J. L. Mock, P. Bletzinger, A. Garscadden, R. A. Gottscho, G. Selwyn, M. Dalvie, J. E. Heidenreich, J. W. Butterbaugh, M. L. Brake, M. L. Passow, J. Pender, A. Lujan, M. E. Elta, D. B. Graves, H. H. Sawin, M. J. Kushner, J. T. Verdeyen, R. Horwath, and T. R. Turner, *Rev. Sci. Instrum.* **65**, 140 (1994).
- [26] C. Garvin, B. E. Gilchrist, D. S. Grimard, and J. W. Grizzle, *J. Vac. Sci. Technol. A* **16**, 595 (1998).

- [27] A. P. Paranjpe, J. P. McVittie, and S. A. Self, *J. Appl. Phys.* **67**, 6718 (1990).
- [28] M. B. Hopkins, W. G. Graham, and T. J. Griffin, *Rev. Sci. Instrum.* **58**, 475 (1987).
- [29] M. B. Hopkins, *J. Res. Natl. Inst. Stand. Technol.* **100**, 415 (1995).
- [30] S. Wolf and R. N. Tauber, *Silicon Processing for the VLSI Era:Vol. 1-Process Technology*, p. 572, Lattice Press, Sunset Beach, CA, 1986.
- [31] B. A. Rashap, M. E. Elta, H. Etemad, J. P. Fournier, J. S. Freudenberg, M. D. Giles, J. W. Grizzle, P. T. Kabamba, P. P. Khargonekar, S. Lafortune, J. R. M. and D. Teneketzis, and F. L. Terry, Jr., *IEEE Trans. Semiconduct. Manufact.* **8**, 286 (1995).
- [32] T. E. Benson, L. I. Kamlet, S. M. Ruegsegger, C. K. Hanish, P. D. Hanish, B. A. Rashap, P. Klimecky, J. S. Freudenberg, J. W. Grizzle, P. P. Khargonekar, and F. L. Terry, Jr., *J. Vac. Sci. Technol. B* **14**, 483 (1996).
- [33] H. H. Goto, H. Lowe, and T. Ohmi, *IEEE Trans. Semiconduct. Manufact.* **6**, 58 (1993).

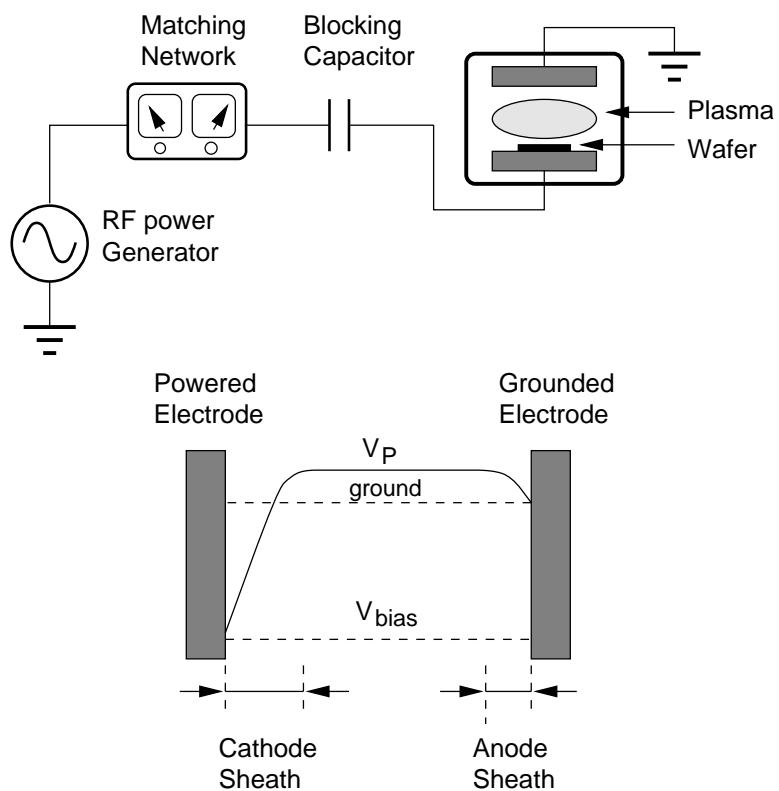


Fig. 1: Schematic of a capacitively coupled asymmetric RIE system and its electrical potential across parallel electrodes when chamber wall and upper electrode are grounded (V_p : plasma potential, V_{bias} : plasma self bias voltage).

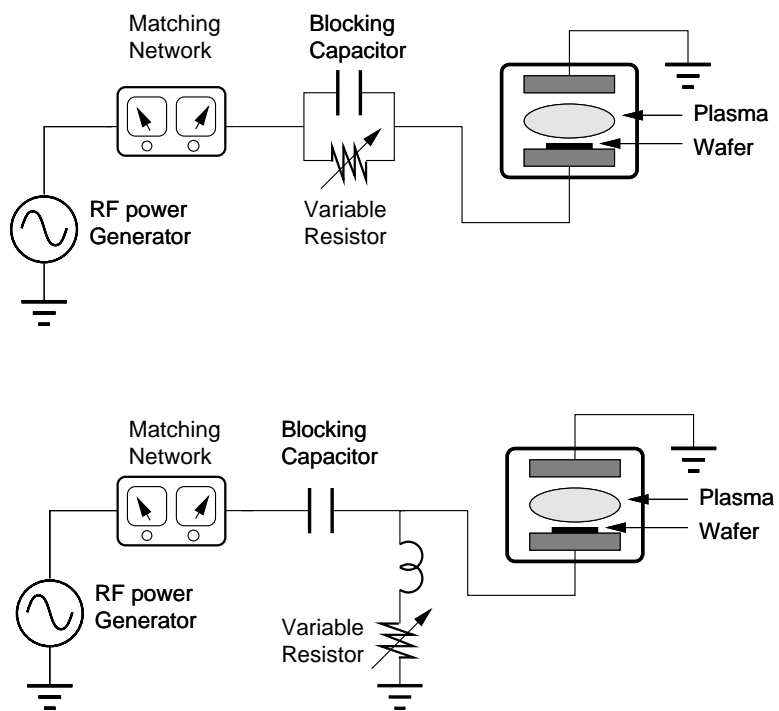


Fig. 2: Schematic of ion energy control using a variable resistor.

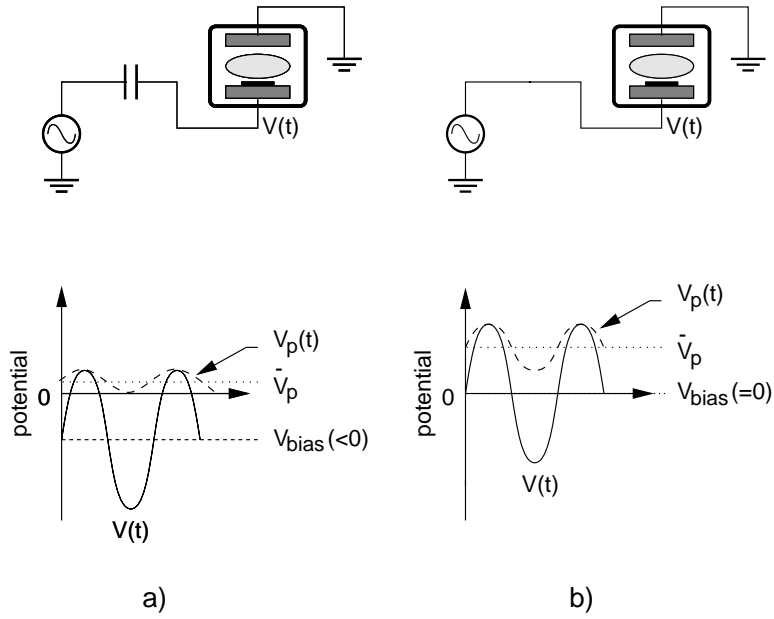


Fig. 3: Illustrative plasma potentials $V_p(t)$ (dashed curves) and powered electrode voltages $V(t)$ (solid curves) for asymmetric electrode area (small powered electrode) for a) capacitively coupled RIE system ($R = \infty$) and b) DC coupled RIE system ($R = 0$).

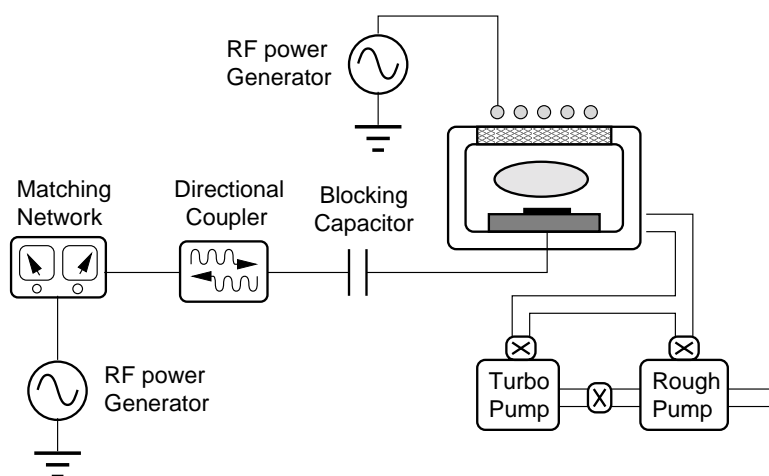


Fig. 4: Schematic of the experimental apparatus.

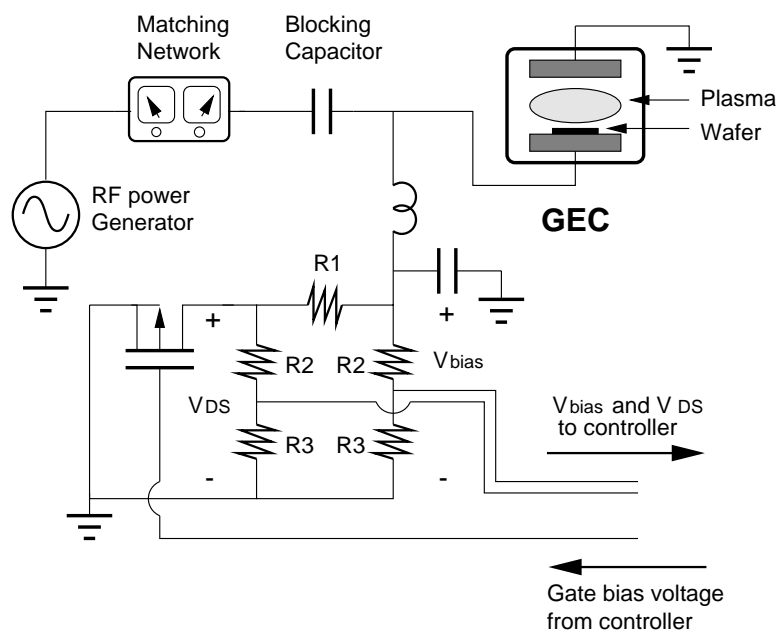


Fig. 5: Schematic of variable resistor for V_{bias} control.

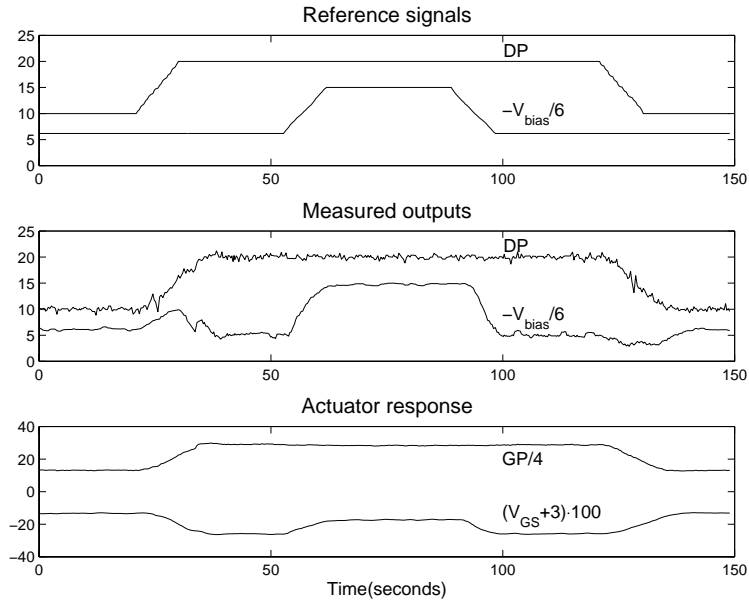


Fig. 6: Experimental response of the GEC following reference signals (DP: Deposited Power (W), V_{bias} : Plasma self bias voltage (V), GP: Generator Power (W), V_{GS} : Gate bias voltage (V), sampling frequency: 4 Hz. The trajectories were scaled to fit on a single plot).

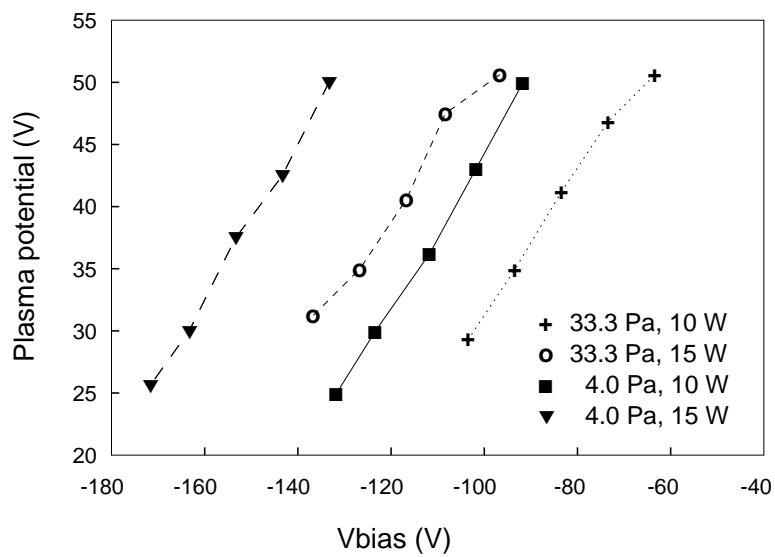


Fig. 7: Plasma potentials of argon plasma at 4.0, 33.3 Pa pressure and 10, 15 W deposited power in GEC.

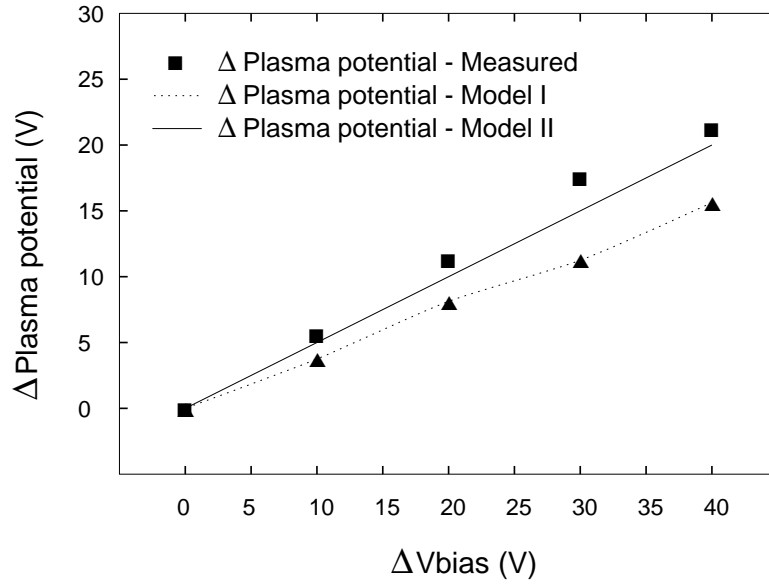


Fig. 8: Plasma potential models at 3.3 Pa, 15 W deposited power, argon plasma ($\Delta V_{bias} = V_{bias} - V_{bias}^{nom}$, $\Delta V_p = V_p - V_p^{nom}$, Model I from (1) and Model II from (8)).

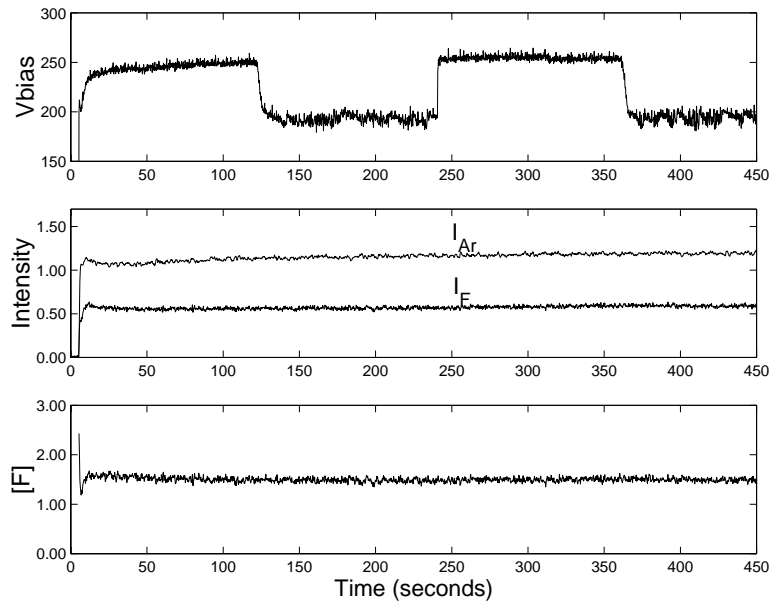


Fig. 9: Fluorine concentration of CF_4 with 5.19% pre-mixed argon plasma with 4.0 Pa pressure, 30 sccm flow rate and 500 W deposited power in an AME-8300 RIE system under V_{bias} control.

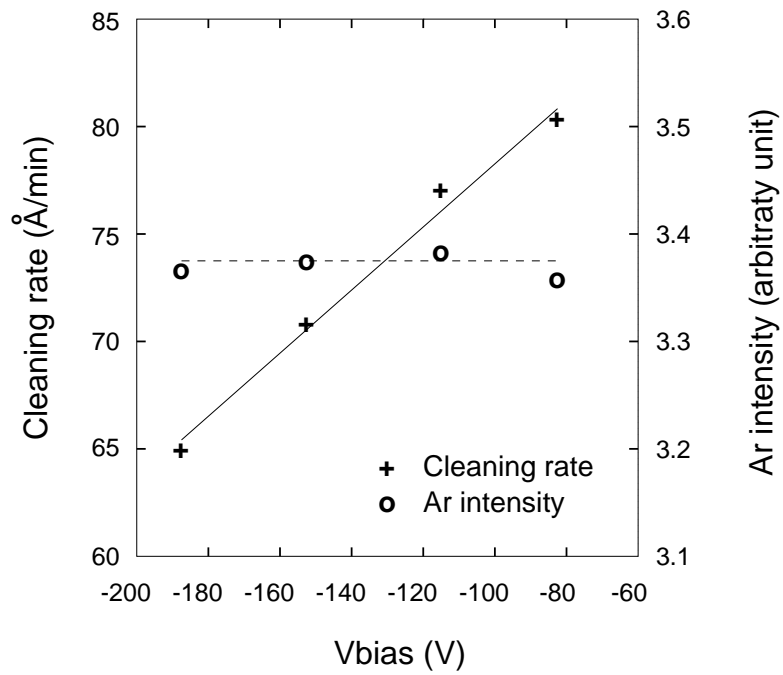


Fig. 10: Cleaning rate with 10 sccm O_2 and 10 sccm argon plasma with 4.0 Pa, 250 W deposited power in AME-8300 RIE system. The solid and dashed lines represent a linear fit to the data.